Geophysical Magnetic Data Analyses of the Geological Structures With Mineralization Potentials Over the Southern Part of Kebbi, NW Nigeria

Article *in* Mining Science · May 2023

DOI: 10.37190/msc222911

CITATION
1

READS
199

4 authors, including:

Abdulrahaman Idris Augie
Federal University Birnin Kebbi, Kebbi State Nigeria
36 PUBLICATIONS **79** CITATIONS
SEE PROFILE

Kazeem Adeyinka Salako
Federal University of Technology Minna
54 PUBLICATIONS **178** CITATIONS
SEE PROFILE

Adewuyi Abdulwaheed Rafiu
Federal University of Technology Minna
33 PUBLICATIONS **94** CITATIONS
SEE PROFILE

Mining Science, vol. 29, 2022, 179–203

www.miningscience.pwr.edu.pl

Mining Science

(Previously Prace Naukowe Instytutu Gornictwa Politechniki Wroclawskiej, ISSN 0370-0798)

ISSN 2300-9586 (print)
ISSN 2353-5423 (online)

Received January 10, 2022; Reviewed; Accepted September 21, 2022

GEOPHYSICAL MAGNETIC DATA ANALYSES OF THE GEOLOGICAL STRUCTURES WITH MINERALIZATION POTENTIALS OVER THE SOUTHERN PART OF KEBBI, NW NIGERIA

Abdulrahaman Idris AUGIE[1, 2]*, Kazeem Adeyinka SALAKO[2], Adewuyi Abdulwaheed RAFIU[2], Mufutau Owolabi JIMOH[3]

[1] Department of Applied Geophysics, Federal University Birnin Kebbi, 860101, Nigeria
[2] Department of Geophysics, Federal University of Technology Minna, 920101, Nigeria
[3] Department of Geology, Federal University of Technology Minna, 920101, Nigeria

Abstract: This study used geophysical data analysis to map and provide useful estimates of the geometry, depth, and magnetization of the magnetic sources, as a continuation and improvement over the earlier analyses in the area. Fugro airborne surveys collected aeromagnetic data for the Nigeria Geological Survey Agency (NGSA) between 2009 and 2010. The study area's data were processed and analyzed using an improved tilt derivative (TDR) technique and 2D magnetic structural modelling. The result of TDR reveals the horizontal location and extent of the edges of various magnetic sources that formed lineaments. The results from 2D modelling for the selected profiles (PI, P2, P3, P4, and P5) identify zones with a high magnetic anomaly responding to fractures. These fracture regions of the basement complex area could be caused by fault/shear zones. Fault-induced areas on these sub-basin floors are important hosts for hydrothermal mineralization. In comparison to the geological setting, these regions are underlain by quartz-mica schist, biotite-hornblende, granite, biotite, gneiss, diorite, migmatite, medium coarse-grained sandstone, ironstones, laterite, siltstones, and clay. These regions could be suitable for mineral exploration and correspond to the Ngaski, Yauri, Magama, Shanga, and Rijau. However, in comparison to the SPI results, the depth/thickness of the sediments that crossed the areas of the sedimentary basin and basement complex zones did not match the results of 2D forward modelling. The SPI technique usually provides an average depth of the magnetic source and is unable to accurately map the undulating basement. While the aforementioned results of 2D forward modelling provide sediment thickness by accurately reflecting basement topography.

***Keywords*:** *2D magnetic modelling, tilt derivative (TDR), source parameter imaging (SPI), structural features and mineralization potentials*

* Corresponding author: ai.augie@fubk.edu.ng (A.I. Augie)

doi: 10.37190/msc222911

1. INTRODUCTION

Subsurface structural analysis is critical in the exploration of mineral resources (Maghfira and Niasari 2017). Almost all types of mineral deposits and hydrocarbon accumulations are influenced, either directly or indirectly, by some structural focus. This could be on a local or regional scale, at the deposit's crustal level, or at greater crustal depths (Adama et al. 2019). Therefore, understanding the formation, origin, and location of mineral deposits requires an understanding of the structural architecture of a mineralized area, the distribution and orientation of faults and shear zones, their formation and possible reactivation during structural evolution, and the tectonic conditions (Reeves 2005; Danbatta et al. 2008; Adewumi and Salako 2018). Thus, aeromagnetic data can be used to assess structural problems at all scales, including mine and prospect scales. The magnetic character of the geology, survey line spacing, and flying height all influence how much aeromagnetic data can contribute to structural analysis (Adetona et al. 2018). Aeromagnetic interpretations typically include a variety of structure types, such as conformable sedimentary contacts, concordant to discordant intrusive and extrusive contacts, erosional contacts, metamorphic layering, faults, shears, fractures, veins, folds, and so on (Isles and Rankin 2013). Furthermore, the structures in the Nigerian basement complex typically control mineralization and may be well established, necessitating a geophysical approach that depicts potential mineral exploration pathways (Ejepu et al. 2018; Augie and Sani 2020). Accordingly, several field mapping exercises were carried out in the southern part of Kebbi, NW Nigeria, in order to assess the mineralization potential solely based on aeromagnetic data. Earlier qualitative studies in the area (Ramadan and Abdel Fattah 2010; Bonde et al. 2019; Lawali et al. 2020; Lawal et al. 2021) reveal major structural trends oriented along ENE–WSW, NE–SW and E–W directions while minor trends were along NW–SE, NNE–SSW, NNW–SSE and N–S directions of the study area. These results are generally concordant with the main regional structural trend and are dipping to the NW. It is also revealed that the northeastern and southwestern parts of the area are dominated by the basement complex, which may play host to economic minerals. Augie et al. (2021) and Augie et al. (2022) correlated that structures delineated within the area correspond to quartz-mica schist, granite, biotite, gneiss, diorite, medium coarse-grained, and biotite hornblende granite when compared to the geological setting. These are mineral-hosting alteration zones. The regions correspond to the southeast parts of Yauri and Shanga, Fakai, Ngaski, Zuru, Magama, and Rijau, as well as the eastern parts of Wasagu/Danko and Bukkuyum (Fig. 1).

In this article quantitative approach is used to provide useful estimates of the geometry, depth, and magnetisation of the magnetic sources. Magnetic modelling can approximate empirical rules that relate a magnetic body's depth, shape, and magnetization to specific parameters derived from anomaly profile plots (Blakely 1996). The southern part of Kebbi is located in a low latitude zone, and none of the previous researchers used a reduction-to-equator (RTE) filter for centralizing the anomalies. To prevent abnormal

noise in the results of the north-south signal in the data at low latitudes, a separate amplitude must be corrected (Holden et al. 2008; Core et al. 2009) as would be done in RTE filtered data. Major potential field filters previously employed in the area are first and second vertical derivatives (FVD and SVD), as well as analytic signals (AS). These techniques occasionally produce false edges and are less effective in detecting the edge of deep or thin sources associated with minerals. Pham et al. (2019), Pham et al. (2020a), Pham et al. (2020b), Pham (2021), and Pham et al. (2021) recently introduced some new methods for detecting lineaments that perform better as edge detection filters. The tilt derivative (TDR) (Miller and Singh 1994) was introduced and uses the amplitude of the total horizontal derivative to normalize the vertical derivative. This technique was improved further to show the shallow and deep edges at the same time. Geophysical magnetic data analyzes were performed on geological structures with mineralization potentials in the southern part of Kebbi (NW Nigeria). These magnetic studies are magnetic data mapping and 2D magnetic data modelling. The improved TDR technique was used in delineating the lineaments (such as faults, fractures or shears zones) believed to be associated with alteration zones which play an important role in determining mineralization potential zones. The 2D data modelling was used as a continuation of magnetic studies as improvements over the earlier analyses (Augie et al. 2021; Augie et al. 2022). TDR was used to map shallow basement structures and mineral exploration targets. 2D magnetic models (geometric bodies) approximate the real geological body, revealing the area's subsurface structural features. The 2D modelling used in this study combines aeromagnetic, shuttle radar topography mission (SRTM), and geologic grid data to identify regions with overburden thickness associated with different earth materials capable of hosting minerals. Using source parameter imaging (SPI) algorithms, this study also reveals the depth to which miners could access for mineral commodities with strong affinities to the rock types within the geological setting of the study area.

Geologically, the study area is comprised of basement complex rocks and a portion of a sedimentary basin (see Fig. 1). Quartz-mica schist, migmatite, granite, biotite gneiss, diorite, medium to coarse-grained, undifferentiated schist including gneiss, and biotite-hornblende granite were associated with the basement complex regions. Sandstone, siltstones, clay, laterites, undifferentiated schist, and medium coarse-grained schist make up the sedimentary basin regions as shown in Fig. 1 (NGSA, 2006). There are also some metasedimentary regions that contain quartzites, schists, and phyllites, whereas older granites contain granodiorites/or diorites (Augie et al. 2022). Furthermore, dacites/rhyolites overlie and intrude on the basement gneisses, metasediments, and granitic rocks of the southern part of Kebbi (Danbatta 2008). The area also included a brittle fault zone composed of sub-parallel phyllites and deformed and undeformed quartzites, and it is part of the mapped Anka transcurrent fault, which is referred to as a possible Pan-African crustal suture (Danbatta 2005). Due to high magnetic anomalies in the region, the southern part of Kebbi is strongly associated with the edge of the magnetic structures (Lawal et al. 2021). When compared to the geological setting of the area, this is usually associated

with the presence of ferromagnetic, Fe-bearing rocks with some felsic minerals (Augie et al. 2022). In this study, geophysical data from the magnetic method and the 2D magnetic modelling technique were used to map the structures that may host minerals. As a continuation and improvement on previous analyses in the area, these methods were used to provide useful estimates of the geometry, depth, and magnetization of the magnetic sources associated with mineralization potential zones.

2. THEORETICAL FRAMEWORK AND PROCEDURES

2.1. REDUCTION TO MAGNETIC EQUATOR (RTE) TECHNIQUE

The study area is located in low-inclination magnetic equatorial zones (low latitudes). RTE techniques usually has an amplitude component [sin(*I*)] and a phase component [*i*cos(*I*) cos(*D* – *θ*)]. The values are always synchronized and given by (Holden et al. 2008 and Core et al. 2009).

$$L(\theta) = \frac{[\sin(I) - i\cos(D-\theta)]^2 \times [-\cos^2(D-\theta)]}{[\sin^2(Ia) + \cos^2(Ia)\cos^2(D-\theta)] \times [\sin^2(I) + \cos^2(D-\theta)}, \text{ if } (|la| < I),\ la = 1 \tag{1}$$

where: *I* is geomagnetic inclination in [degrees], *D* is geomagnetic declination in [degrees azimuth] and *Ia* is inclination for amplitude correction (never less than 1), $L(\theta)$ is non-dimensional and is a multiplier that must scale down or up some magnetic field anomaly. Equation (1) gives the field strength that is usually required for apparent susceptibility calculation.

The TMI map was reduced to the magnetic equator using this equation to produce anomalies that do not depend on the inclination and declination of the magnetized body, the local earth's field, and the body's orientation with respect to the magnetic north.

2.2. TECHNIQUE TILT DERIVATIVE (TDR) TECHNIQUE

For mapping shallow basement structures and mineral exploration targets, the tilt derivative and its total horizontal derivative are useful (Miller and Singh 1994; Thurston and Smith 1997).

The tilt derivative (TDR) is defined as

$$\text{TDR} = \tan^{-1}\left(\frac{\text{VDR}}{\text{THDR}}\right). \tag{2}$$

DR and THDR are the first vertical and total horizontal derivatives, respectively, of the total magnetic intensity anomaly field *T*.

$$\mathrm{VDR} = \frac{dT}{dz}, \tag{3}$$

$$\mathrm{THDR} = \sqrt{\left(\frac{dT}{dx}\right)^2 + \left(\frac{dT}{dy}\right)^2}. \tag{4}$$

The total horizontal derivative of the tilt derivative is defined as:

$$\mathrm{HD\_TDR} = \sqrt{\left(\frac{d\mathrm{TDR}}{dx}\right)^2 + \left(\frac{d\mathrm{TDR}}{dy}\right)^2}. \tag{5}$$

HD_TDR is in units of radians/distance.

Consequently, these equations were used to evaluate this study. The following steps were used for calculating the TDR grid: firstly, aeromagnetic data from a reduced RTE anomaly grid were inputted named as TILTDRV.IN and the output tilt derivative grid (TDR) was named the parameter TILTDRV.OUT. Likewise, the output horizontal derivative of the TDR grid (HD-TDR) was named TILDTDRV.OUT2. The parameter of the *z*-derivative was computed using the fast Fourier transform (FFT) and was named TILTDRTV.METHOD. Thus, the TDR map was prepared.

2.3. SOURCE PARAMETER IMAGING (SPI) TECHNIQUE

The SPI method distinguishes and characterizes regions of deep magnetic sources from those of shallow magnetic sources, as well as determining the magnetic source's depth (Thompson 1982). The depth estimate is unaffected by magnetic inclination, declination, dip, strike, or remanent magnetization (Odidi et al. 2020). The SPI technique is based on a step-type source model (Smith et al. 1998) given as.

$$D = 1/k_{\max}, \tag{6}$$

where $k_{\max}$ represents the peak value of k (local wave number) which is located over the step source with

$$k = \sqrt{\left(\frac{dA}{dx}\right)^2 + \left(\frac{dA}{dy}\right)^2}, \tag{7}$$

where A is the tilt derivative (TDR). Maximum value of k occurs at the tips of the wavelength and so capable of mapping structural boundaries.

This study/article made use of these equations. Using the standard Montaj filters, the SPI menu allows to computation of the two horizontal derivative grids (*dx* and *dy*) in the space-domain and the first vertical derivative grid (*dz*) in the frequency-domain. The *dx*, *dy*, and *dz* were computed by inputting the RTE grid. The resultant *dx*, *dy*, and *dz* grids

were input to calculate the SPI grid. The output lines and channels reveal the database consisting of *X* and *Y* coordinates of the solution points which are saved in the specified line. The corresponding depths are saved in a channel called SPI value. Thus, the depth values were further griddled, and the resultant SPI map was prepared for this article.

2.4. 2-D QUANTITATIVE MODELLING

The subsurface configuration of magnetic units can be determined using modelling techniques. The most common method is forward modelling, which involves using an initial guess of the shape and magnetization to calculate a magnetic anomaly, comparing the calculated anomaly to the observed anomaly, and modifying the shape and magnetization to improve agreement between the two. This uses standard forward modelling methods to approximate subsurface geology with horizontal tabular prisms characterized as model blocks in the 2D cross-section. The model blocks had to be consistent with the mapped geologic units. The model bodies' geometries were determined using a series of forward and inverse calculations to match model anomalies with observed anomalies within the limits imposed by surface geology and rock property data useful for estimating the horizontal extent of buried sources (Talwani et al. 1959; Blakely and Connard 1989). Typically, the modelling procedure can be automated using one of two types of inverse modelling techniques: (a) if the source's bounding shape is known, the distribution of magnetization within the source can be determined using least-squares or Fourier--transform techniques; and (b) if simplifying assumptions for the distribution of magnetization can be developed, the shape of magnetic sources can be automated (Bott 1967; Parker 1973).

For this study, the steps used include calculation, comparison and adjustment as continuously until the calculated and observed anomalies are in satisfactory agreement using the gravity/ magnetic system (GM-SYM) in Oasis Montaj software. The steps taken using the Oasis Mantaj were first assembling the RTE, SPI, SRTM, and Geologic grids from the grid profile menu. The line names were given as profiles 1, 2, 3, 4, and 5, with a sample interval of 200 m. The method used to set profile coordinates was digitizing from a map. The profiles, on the other hand, were extracted from RTE, SPI, SRTM, and geologic grids perpendicular to the area's geological structures. The elevation of each profile was calculated using data tools from the SRTM database. GX system was used to load the GM-SYS menu for 2D magnetic modelling. The obtained RTE, elevation, and SRTM grids were inputted into the system, and the root name for the models was named "models". The results from GM-SYS reveal the model of each profile. The adjustment of the calculated and observed curves of the models was made until they matched each other. This will approximate the real geological body and aid in the discovery of subsurface structural features. The models provided useful estimates of the geometry, depth, and magnetization of magnetic sources.

3. THE STUDY AREA

This research focuses on the southern part of Kebbi state, as well as parts of the Zamfara and Niger states, NW Nigeria. The region is located between latitudes 10°30′0″N and 12°0′0″N, and longitudes 4°0′0″E and 5°30′0″E. It covered the areas of Zuru, Ngaski, Yauri, Shanga, Sakaba, Fakai, Danko/Wasagu, Koko Besse, Maiyama, Bagudo, Suru, Kebbe, Bukkuyum, Gummi, Agwara, Rijau, Borgu, and Magama (see Fig. 1).

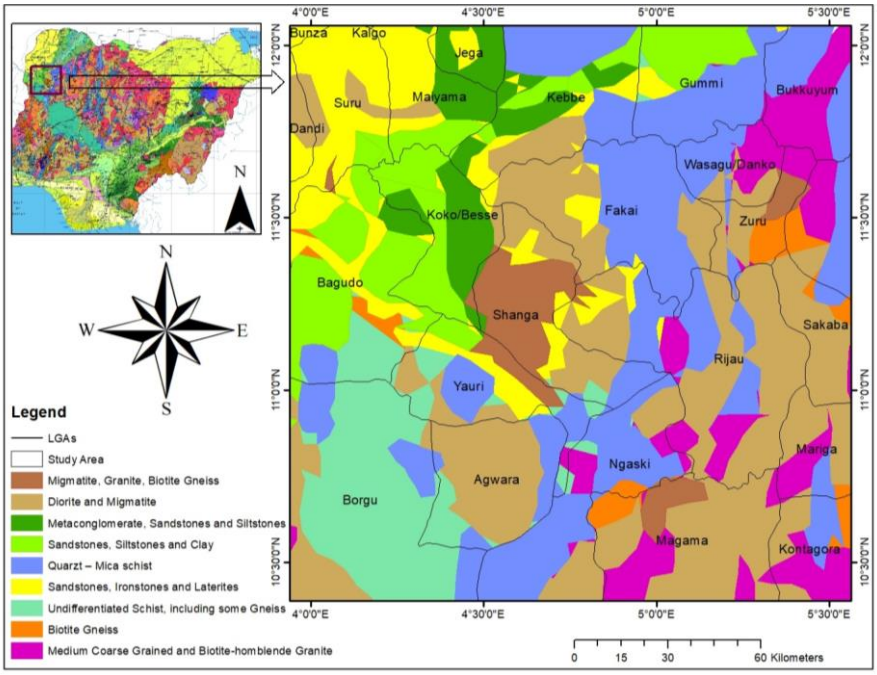

Fig. 1. Location and geological map of the study (Augie et al. 2022)

The area has an elevation ranges from 148.40 m to 396.10 m (Fig. 2). The areas marked with light blue to dark blue in Suru, Dandi, Magama, Bagudu, Koko/Besse, Shanga, Yauri, Agwara, Ngaski, and parts of Kebbe, Fakai, Borgu, and Magama had the lowest value. The regions marked with yellow to pink had the highest value. Jega, Gummi, Bukkuyum, Wasagu/Danko, Zuru, Sakaba, Rijau, Mariga, Kontagora, and parts of Kebbe, Fakai, Borgu, and Magama are among these areas (see Fig. 2). Climatically, two seasons are observed; the first is the winter season, which begins in March and ends in October each year. Second, the harmattan season runs from November to March each year. As shown in Fig. 2, the topographical elevation ranges from 148.40 m in the val-

leys to 396.10 m on the hills. The area's valleys and hills are associated with basement and sedimentary zones, respectively.

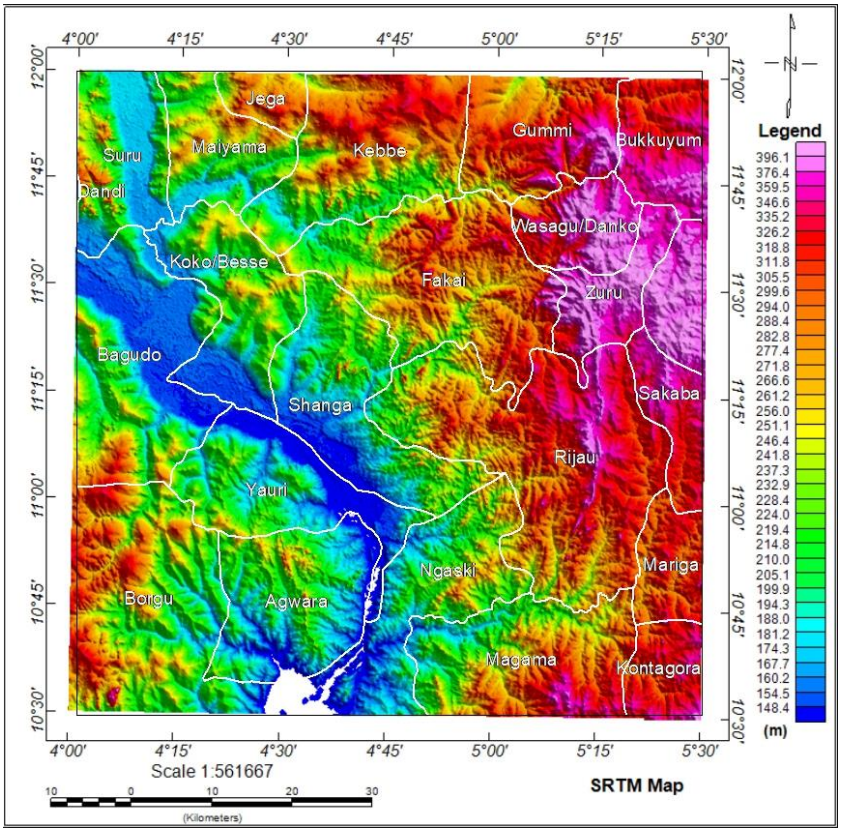

Fig. 2. Digital elevation model of the study area showing the topography

Figure 2 depicts the high-elevation regions in a red-pink colour. When compared to the geological setting of the area (Fig. 1), they fall under the basement complex. These areas were associated with quartz-mica schist, migmatite, granite, biotite gneiss, diorite, medium- to coarse-grained, undifferentiated schist including gneiss, and biotite-hornblende granite. The low-elevation zones are denoted by a green-blue colour. When compared to the geological setting, the regions are part of a sedimentary basin. The basin's earth materials include sandstone, siltstones, clay, laterites, undifferentiated schist, and medium coarse-grained schist.

However, the regions of the basement complex containing the aforementioned earth material usually exhibit significant positive magnetic susceptibility, which corresponds to the presence of ferromagnetic minerals such as gold. Mafic and ultramafic

rocks with ferromagnetic properties are more likely to contain Fe-bearing minerals (gold minerals). As a result of the types of rock formations highlighted in these areas, the regions are suitable for this study. The carbonate content of the depositional environment can strongly influence the portion of the sedimentary basin in a given zone, and the carbonate species are usually strongly dependent on both sedimentary facies and sediment provenance.

4. MATERIALS AND METHOD

In this study, acquired aeromagnetic, shuttle radar topography mission, and geologic grid data were used covering the southern part of Kebbi and its environs (study area). Fugro airborne surveys collected the aeromagnetic data for the Federal Government of Nigeria between 2009 and 2010. The Nigeria Geological Survey Agency (NGSA) is the custodian of data grids. Half-degree grids are obtained are: Grids 72_(Giru), 73_(Eokku), 74_(Donko), 95_(Kaoje), 96_(Shanga), 97_(Zuru), 117_(Konkwesso), 118_(Yelwa), and 119_(Chifu) were acquired. The data are high-resolution aeromagnetic (HRAM). High--resolution aeromagnetic (HRAM) data are commonly defined as data collected at a flight line spacing of 800 m or less, at flight heights of 150 m or less, at 15 m or less sample spacing along flight lines and at better than 0.1 nT accuracy. The present survey does fall under this definition since the flight line spacing is 500 m (<800 m specification for HRAM) and the data recording interval is less than 0.1 s or less than 7 m (<15 m requirement for HRAM) and so all criteria for HRAM were satisfied in these data. Flight line spacing (500 m), terrain clearance (80 m), tie line spacing (2000 m), flight direction is NW–SE, and tie line direction is NE–SW. The acquired data were corrected by removing the geomagnetic gradient (Definitive Geomagnetic Reference Field, DGRF) using the main/core field. The generated core fields (DGRF for the 2010 epoch period) are subtracted from the grid values (TMI) to give the magnetic anomaly (TMI anomaly). TMI anomaly map was reduced to the magnetic equator in order to reveal the effects of rock materials polarized by the horizontal component of the Earth's magnetic field and therefore centralizing the field data on the causative materials.

Finally, 2D magnetic evaluation was performed by selecting 5 magnetic profile lines across the RTE map of the study area. This uses standard forward modelling methods (Talwani et al. 1959; Talwani and Heirtzler 1964) to approximate subsurface geology as model blocks in the 2D cross-section. The technique employed magnetic, shuttle radar topography mission (SRTM) and geologic grid data obtained from NGSA. A series of forward and inverse calculations were used to match model anomalies with observed anomalies within the constraints imposed by surface geology and rock property data. The parameters that define the model are adjusted, and the anomaly is recalculated until the calculated and observed anomalies give a plausible geologic model source. This

entails making numerical estimates of the depth and dimensions of the sources of anomalies until the models revealed the geological body associated with the area's subsurface structural features.

5. RESULTS AND DISCUSSION

5.1. TMI AND RTE RESULTS

Figure 3 shows a colour representation of the TMI map of the study area. This TMI was transformed into a TMI anomaly by subtracting the generated core fields (DGRF for the epoch period) from it. TMI anomalies were then further reduced to the magnetic equator (RTE). The resultant composite colour depicting RTE anomalies is given in Fig. 4. This is primarily used in this study to reveal the magnetic characteristic of the various lithological units in the area.

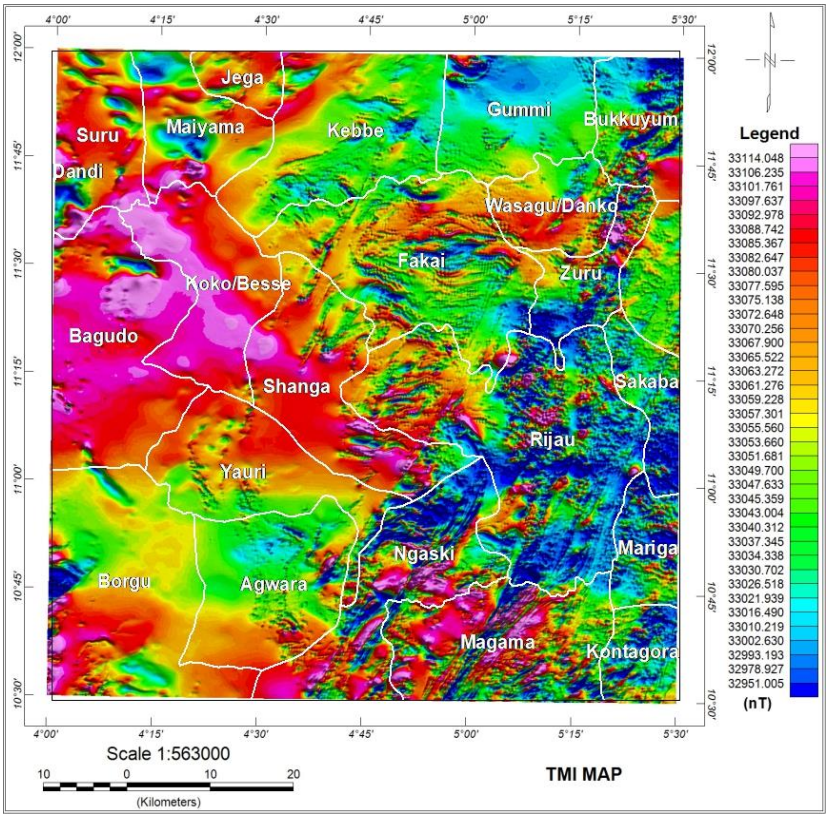

Fig. 3. Total magnetic intensity (TMI) map of the study area

The magnetic signatures range from a low magnetic anomaly to a high magnetic anomaly. Anomalies ranging from –660.764 nT to –449.618 nT exhibit a high magnetic trend, which is signified by a red or pink colour. These regions are corresponded to the Yauri, Ngaski, Shanga, Bagudo, Koko/Besse, Borgu, Agwara, Magama, Kontagora, and some part of Mariga. Areas with low magnetic anomalies, indicated in blue, ranging from –773.258 nT to –882.685 nT. These zones correspond to the Gummi, Bukkuyum, Kebbe, Jega, Wasagu/Danko, Zuru, and Sakaba. The regions moderate magnetic trends indicated in green, ranged from –763.974 nT to –679.219 nT. These zones are correlated to Suru, Dandi, Maiyama, Fakai and Rijau (see Figure 4). Thus, low and high regions are distinguished by different rock formations that result in variations in the magnetic susceptibility of the rocks within the area. The susceptible rocks typically occur at depths shallower than the curie point isotherm. The high negative values indicate high magnetic susceptibility zones as the magnetic equator is a zone of zero inclination and all rocks are polarized by the horizontal component of the Earth's magnetic field which

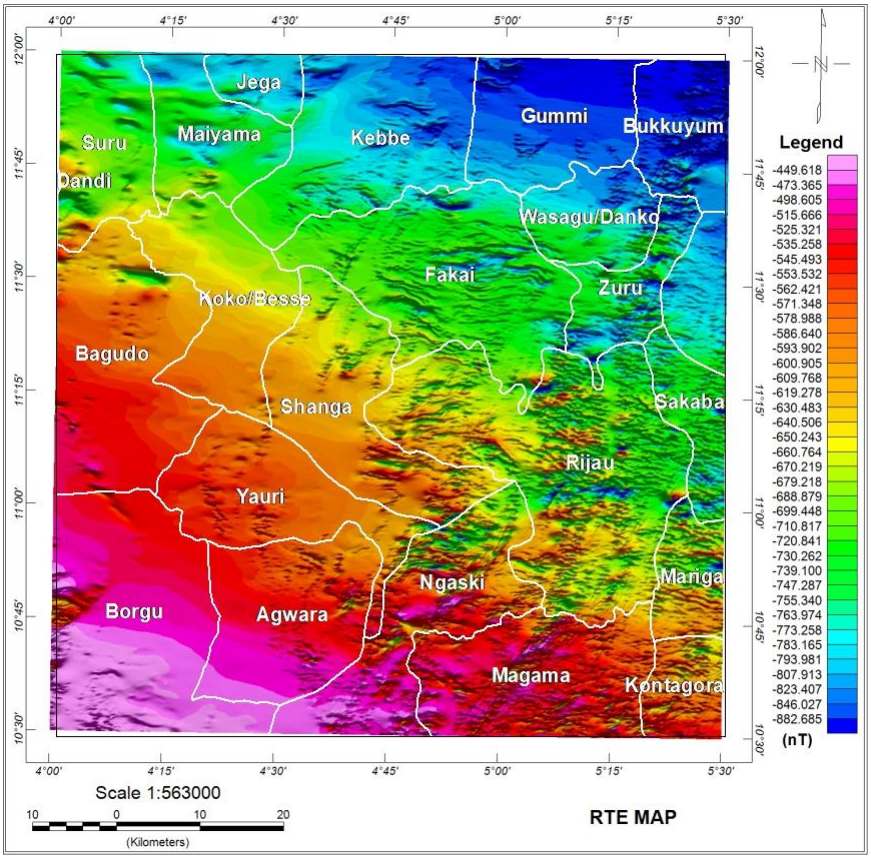

Fig. 4. Reduced to equator (RTE) map of the study area

usually opposes the rock magnetization. The resultant anomaly after the removal of the crustal field and other temporal effects from the measured field is usually negative over magnetic materials.

5.2. TDR RESULT

Figure 5 shows the TDR map of the area generated from RTE anomalies (Fig. 4). The map reveals the horizontal location and extent of the edges of various magnetic sources that formed lineaments. The edges of the shallow and deep sources of magnetic anomalies were more pronounced. The major structures are seen within the SE parts of Yauri and Shanga, Fakai, Ngaski, Zuru, Magama, Rijau, Wasagu/Danko, and Bukkuyum. These structures revealed the spatial location of the magnetic source edges. When compared to the geological setting of the area, the regions are underlain by granite, rhyolite, biotite-granite, meta-conglomerate, quartz-mica schist, migmatite, and gneiss. These structures might be potential hosts for minerals.

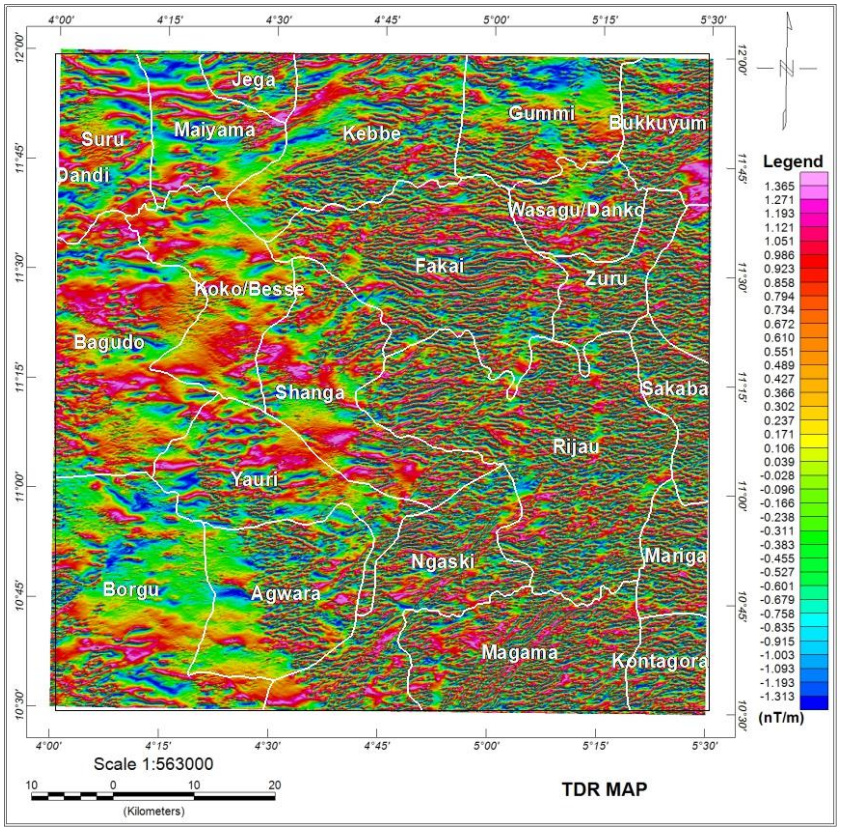

Fig. 5. Tilt derivative (TDR) map of the study area

5.3. SPI RESULT

Figure 6 revealed the depth to magnetic sources as well as the depth to basement rock contact, fractures, or faults with dykes. Examining closely the depths are divided into three categories: <137 m, identified with a pink colour, 150 m to 303 m, identified with a yellow/green colour, and above 665 m, identified with a blue colour. The obtained SPI depth map aided in specifying the depth of the causative body boundaries and trends of the structures shown and in Fig. 7. The pink zones <137 m depth correspond to fault/ structural trend regions identified in the SE parts of Yauri and Shanga, Fakai, Ngaski, Zuru, Magama, Rijau, the eastern part of Wasagu/Danko, and Bukkuyum. The blue zones >1000 m depth correspond to portion sedimentary basin. These regions identified in the Suru, Dandi, Maiyama, Bugudo, Jega, Koko/Besse, Borgu and some parts of shanga, Yauri and Kebbe.

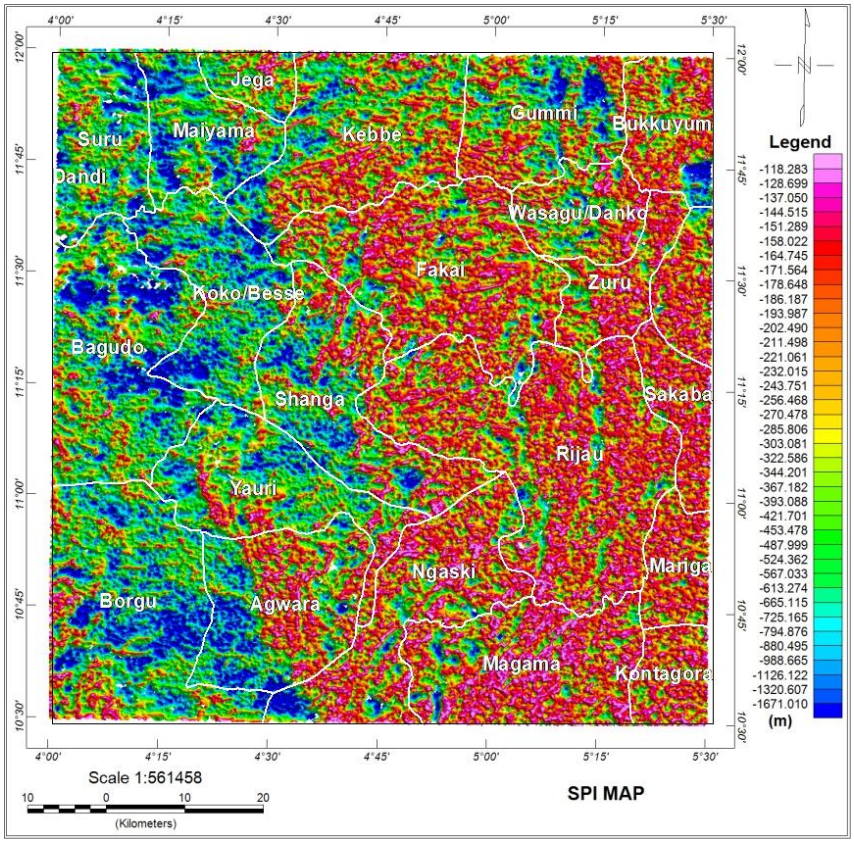

Fig. 6. Depth estimates from source parameter imaging (SPI)
of the RTE anomaly map of the study area

5.4. 2D MAGNETIC MODELLING

The five profiles for the modelling are selected to run perpendicular to the structural trend pictured from the TDR technique (Fig. 5) and the geological setting of the area (Fig. 1) shown in Fig. 7. These would aid in estimating subsurface structures that might be potential hosts for mineral resources. Results from 2D magnetic models for the five profiles are interpreted in terms of the geological setting of the area and susceptibility of rock as given in Figs. 8–12. The results of the 2D forward modelling are summarized in Table 1. The table shows the mineralization potential zones of the study area for 2D modelling profiles P1, P2, P3, P4, and P5. It included the locations, distances, and depths/thickness of the area's suitable mineralization exploration potential zones. These areas correspond to the Ngaski, Shanga, Rijau, Magma, Zuru, the eastern part of Yauri, and Kontagora.

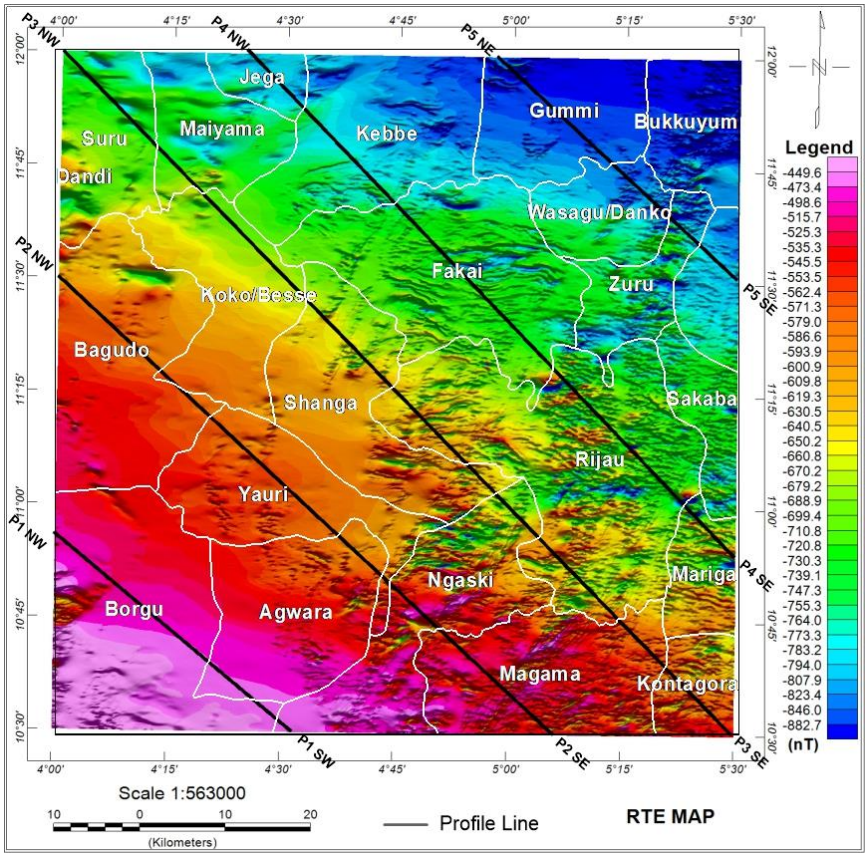

Fig. 7. Line profiles across the RTE map of the study area

Table 1. Summary of results obtained from the 2D forward modelling

S/N	Profile	Location	Lateral length [km]	Depth/ thickness [km]	Rock compositions	Probable mineralization potential remark
1	P1	NE part of Borgu	0.00–34.00	0.00–0.60	quartz-mica schist, undifferentiated schist including some gneiss	No
		Northern part Agwara	35.00–54.00	0.00–1.40	undifferentiated schist including some gneiss, quartz-mica schist	No
		SE part of Ngaski	55.00–80.00	0.00–1.80	quartz-mica schist	Yes
2	P2	NE part of Bagudu	0.00–45.00	0.00–0.20	sandstone, ironstones, laterite, siltstones and clay	No
		NE part of Yauri	46.00–87.00	0.00–0.60	sandstone, ironstones, laterite, siltstones and clay	No
		Eastern part of Borgu	88.00–105.00	0.00–0.60	sandstone, ironstones, laterite, siltstones and clay	No
		Eastern part of Yauri	106.00–120.00	0.00–2.20	medium coarse grained, biotite-bornblande granite	Yes
		NE part of Ngaski	121.00–140.00	0.00–2.00	medium coarse grained, biotite-bornblande granite, sandstone, ironstones, laterite, siltstones and clay	Yes
		SW part of Magama	141.00–165.00	0.00–1.80	biotite gneiss, diorite, migmatite, medium coarse grained, biotite-bornblande granite	Yes
3	P3	SE part of Suru	0.00–14.00	0.00–0.30	sandstone, ironstones, laterite, siltstones and clay	No
		NE part of Koko/Besse	15.00–83.00	0.00–0.30	sandstone, siltstones, clay and metaconglomerate	No
		NE part of Shanga	84.00–98.00	0.00–0.60	migmatite, granite, biotite and gneiss	Yes
		SW part of Rijau	99.00–119.00	0.00–1.20	diorite, migmatite and quartz mica-schist	Yes
		Eastern part of Shanga	120.00–133.00	0.00–2.40	quartz mica-schist	Yes
		Eastern part of Ngaski	134.00–147.00	0.00–3.00	diorite, migmatite, medium coarse grained and biotite	Yes
		Southern part of Rijau	148.00–182.00	0.00–3.60	diorite, migmatite, medium coarse grained and biotite	Yes
		Eastern part of Magama	183.00–203.00	0.00–4.20	migmatite, granite, biotite and gneiss	Yes
		Kontagora	204.00–231.00	0.00–6.60	diorite, migmatite, medium coarse grained and biotite	No

4	P4	Southern part of Jega	0.00–20.00	0.00–0.20	metaconglomerate, sandstone, siltstones, ironstones, laterite and clay	No
		SW part of Kebbe	21.00–50.00	0.00–0.20	metaconglomerate, sandstone, siltstones, ironstones, laterite, clay, diorite and migmatite	No
		Fakai	51.00–110.00	0.00–1.20	diorite, migmatite and quartz-mica schist	No
		NE part of Rijau	111.00–145.00	0.00–0.22	diorite, migmatite, quartz-mica schist, medium coarse grained and biotite hornblende granite	Yes
		Northern part of Magama	146.00–170.00	0.00–1.80	diorite, migmatite, quartz-mica schist, medium coarse grained and biotite hornblende granite	Yes
5	P5	SW part Gummi	0.00–32.00	0.00–1.00	sandstone, siltstones, clay and quartz-mica schist	No
		NE part of Wasagu/Danko	33.00–50.00	0.00–1.80	quartz-mica schist, diorite and migmatite	No
		NE part of Zuru	51.00–63.00	0.00–1.60	quartz-mica schist, diorite, migmatite, coarse grained and biotite bornblende	Yes
		Eastern part of Sakaba	64.00–80.00	0.00–2.60	diorite and migmatite	No

5.4.1. PROFILE 1 (P1)

The 2D forward modelling of magnetic data for P1 is shown in Fig. 8. The profile runs from the NW part of Borgu to the SE part of Ngaski (see Fig. 7). The subsurface features of P1 could be sectionalized into sediments and the basement. The sediment thickness varies over the basement configurations. The maximum depth/thickness of the sediment section that crossed the sedimentary basin is 1.4 km. These areas corresponded to the northwest portion of Borgu and the northern portion of Agwara. The maximum depth/thickness of the sediment section that crossed the basement complex zone is 1.8 km. These zones corresponded to the SE part of Ngaski. In comparison to the geological setting of the area (Fig. 1), the sediments section was made of different earth materials as given in Table 1. The model, however, is based on the magnetic anomaly curves obtained, and these fracture curves were characterized by a high magnetic anomaly (–460.00 nT/m) shown in the SE part of Ngaski. The pattern of this curve is in response to fault or shear zones. In these fault-induced areas, fault features on the sub-basin floor may be important hosts for hydrothermal mineralization. These areas could be potential mineral exploration targets.

The thickness of the sediments (1.4 km) is insufficient for hydrocarbon maturation in the profile portion of the sedimentary basin. According to Wright et al. (1985), the min-

imum thickness for the concealment of hydrocarbons is about 2.3 km; the results obtained fall short of this standard. This implies that hydrocarbon accumulation is not a viable option. In comparison to the SPI results, the depth/thickness of the sediments that crossed the aforementioned zones of the sedimentary basin and basement complex is 1.671 km and <0.137 km, respectively. The results of SPI did not match the results of 2D forward modelling, because of it various impediments. It only provides average depth of magnetic source, and it is unable to accurately map the undulating basement. This explains why 2D forward modelling was used in this study to provide sediment thickness while accurately reflecting basement topography.

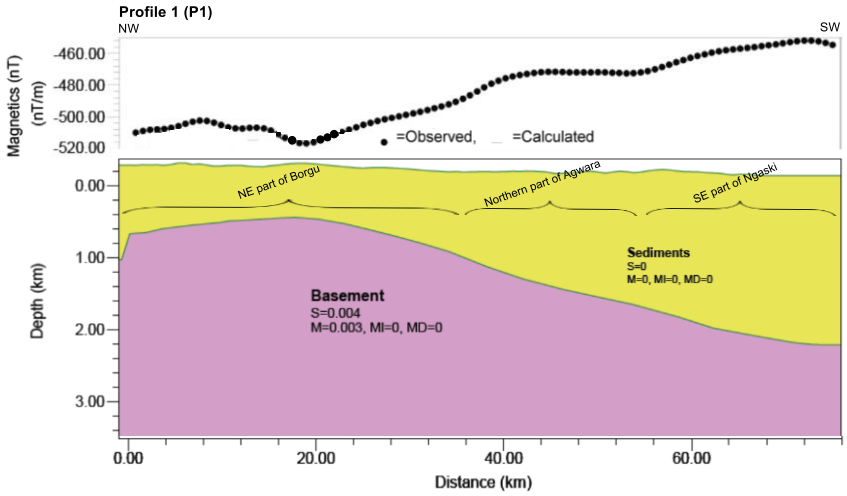

Fig. 8. 2D iterative inversion model of magnetic data for profile one

5.4.2. PROFILE 2 (P2)

Figure 9 shows the 2D forward modelling of magnetic data for P2. As shown in Fig. 7, the profile runs from the northeast corner of Bagudu to the southwest corner of Magama. P2's subsurface features can be divided into sediments and the basement. The thickness of the sediment varies according to the configuration of the basement. The maximum depth/thickness of the sediment section that crossed the sedimentary basin is 1.5 km. These areas corresponded to the northeastern part of Bagudo, the northeastern part of Yauri, and the eastern part of Borgu. The sediment section that crossed the basement complex zone reached a maximum depth/thickness of 2.6 km. These zones corresponded to the eastern portion of Yauri, the northeast portion of Ngaski, and the southwest portion of Magama. In comparison to the geological setting (Fig. 1), the sediments section was composed of various earth materials, as shown in Table 1. The model, on the other hand, is based on the magnetic anomaly curves that were obtained. A fracture curve identifies a high magnetic anomaly (–520.00 nT/m) in the eastern part of Yauri, the

northeastern part of Ngaski, and the southwest part of Magama. This curve's pattern is caused by faults or shear zones. Fault features on the sub-basin floor may be important hosts for hydrothermal mineralization in these fault-induced areas. These areas may be suitable for mineral exploration. The thickness of the sediments (1.5 km) is insufficient for hydrocarbon maturation in the profile of the sedimentary basin. The minimum thickness for the concealment of hydrocarbons, according to Wright et al. (1985), is approximately 2.3 km; the results obtained fall short of this standard. This implies that accumulating hydrocarbons is not feasible. In comparison to the SPI results, the depth/thickness of the sediments that crossed the aforementioned sedimentary basin and basement complex zones is 1.671 km and 0.137 km, respectively. The SPI results did not match the 2D forward modelling results due to a variety of impediments. It only provides an average depth of magnetic source and is unable to accurately map the undulating basement. This explains why, in this study, 2D forward modelling was used to provide sediment thickness while accurately reflecting basement topography.

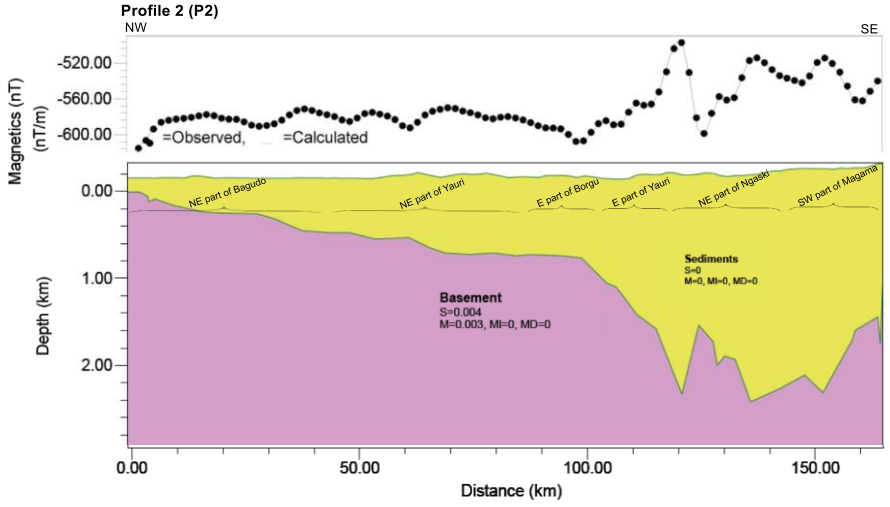

Fig. 9. 2D Iterative inversion model of magnetic data for profile two

5.4.3. PROFILE 3 (P3)

The 2D forward modelling of magnetic data for P3 is shown in Fig. 10. The profile runs from the SE part of Suru to Kontagora, as shown in Figure 7. Sediments and basement are the two subsurface features of the P3. The thickness of the sediment varies according to the basement configuration. The sediment section that crossed the sedimentary basin had a maximum depth/thickness of 0.8 km. These zones correspond to the SE part of Suru, the SW part of Maiyama, and the NE of Ko-

ko/Besse. The depth/thickness of the sediment section that crossed the basement complex zone reached 9.6 km. These zones correspond to the northern part of Shanga, the southern part of Rijau, the eastern part of Ngaski, the southern part of Rijau, the eastern part of Magama, and Kontagora. In comparison to the geological setting (Fig. 1), the sediment section was made up of a variety of earth materials, as shown in Table 1. The model, on the other hand, is based on the obtained magnetic anomaly curves. In the aforementioned basement complex areas, a fracture curve identifies a high magnetic anomaly (–560.00 to –630 nT/m). The pattern of this curve is caused by faults or shear zones. In these fault-induced areas, fault features on the sub-basin floor may be important hosts for hydrothermal mineralization. These areas could be good for mineral exploration. The sedimentary basin's sediment thickness (0.8 km) is insufficient for hydrocarbon maturation. According to Wright et al. (1985), the minimum thickness for the concealment of hydrocarbons is approximately 2.3 km; the results obtained fall short of this standard. This means that accumulating hydrocarbons is not a viable option. In comparison to the SPI results, the depth/thickness of the sediments that crossed the aforementioned sedimentary basin and basement complex zones is 1.671 km and <0.137 km, respectively. Because of various impediments, the SPI results did not match the results of 2D forward modelling. It only provides an average depth of magnetic source and is unable to map the undulating basement accurately. This explains why in this study, 2D forward modelling was used to provide sediment thickness while accurately reflecting basement topography.

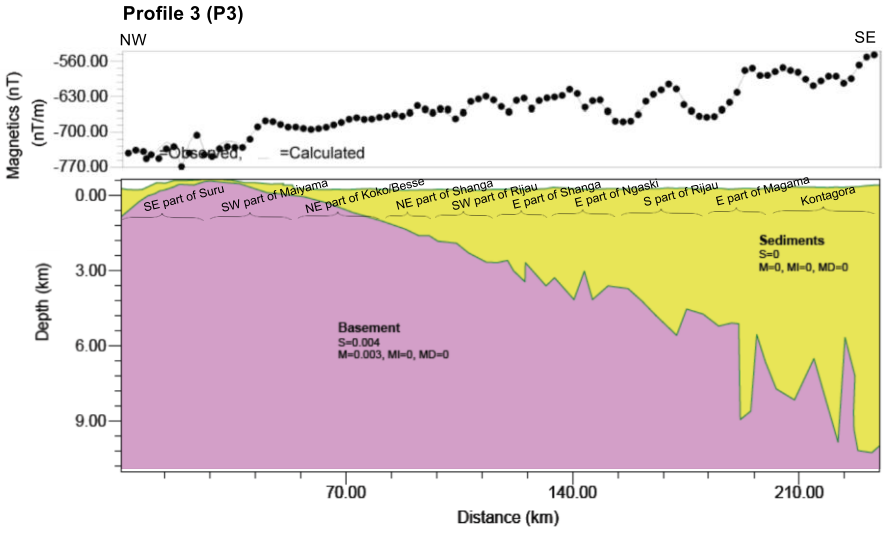

Fig. 10. 2D Iterative inversion model of magnetic data for profile three

5.4.4. PROFILE 4 (P4)

Figure 11 illustrates the 2D forward modelling of magnetic data for P4. The profile runs from the southern part of Jega to the northern part of Magama (see Fig. 7). The P4 has two subsurface features: sediment and basement. The thickness of the sediment varies with the configuration of the basement. The maximum depth/thickness of the sedimentary basin section was 1.2 km. These zones correspond to the southern part of Jega, the western part of Kebbe, and Fakai. The sediment section that crossed the basement complex zone reached a depth/thickness of 2.9 km. These zones correspond to the northern and north-eastern parts of Rijau and Magama, respectively. Table 1 shows that, in comparison to the geological setting (Fig. 1), the sediment section was composed of a variety of earth materials. The model, on the other hand, is based on the magnetic anomaly curves that were obtained. A fracture curve identifies a high magnetic anomaly (–700.00 nT/m) in the aforementioned basement complex areas. This curve's pattern is caused by faults or shear zones. Fault features on the sub-basin floor may be important hosts for hydrothermal mineralization in these fault-induced areas. These areas may be suitable for mineral exploration. The sediment thickness (1.2 km) in the sedimentary basin is insufficient for hydrocarbon maturation, as the minimum thickness for hydrocarbon concealment is approximately 2.3 km. This means that accumulating hydrocarbons in the area is not a viable option.

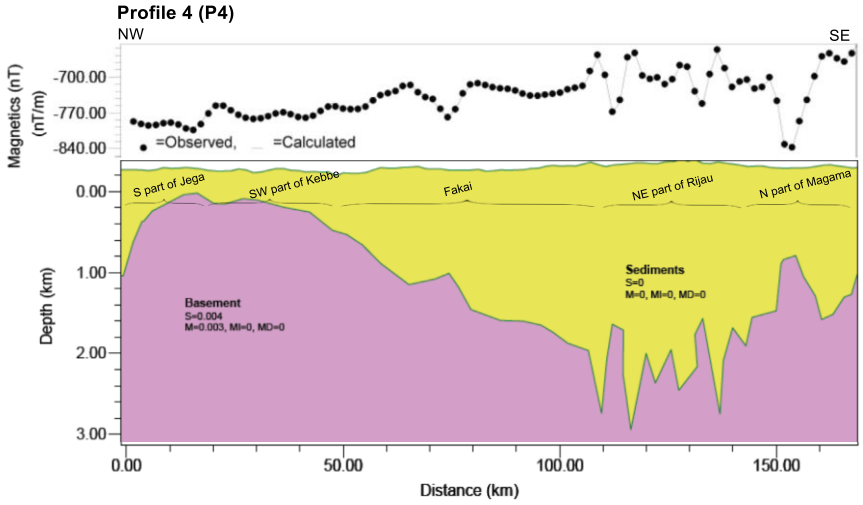

Fig. 11. 2D Iterative inversion model of magnetic data for profile four

5.4.5. PROFILE 5 (P5)

Figure 12 depicts 2D forward magnetic data modelling for P5. The profile runs from the SW part of Gummi to the Eastern part of Sakaba (see Fig. 7). Sediments and basements are two subsurface features of the P5. The thickness of the sediment varies according to the basement configuration. The sedimentary basin section has a maximum depth/thickness of 1.2 km. These zones correspond to the SW part of Gummi. The depth/thickness of the sediment section that crossed the basement complex zone was 2.6 km. These zones correspond to the NW Wasagu/Danko, the NE Zuru, and the eastern Sakaba. Table 1 shows that the sediment section was made up of a variety of earth materials in comparison to the geological setting (Fig. 1). The model, on the other hand, is based on the obtained magnetic anomaly curves. In the Zuru, a fracture curve identifies a high magnetic anomaly (–800.00 nT/m). The pattern of this curve is caused by faults or shear zones. In these fault-induced areas, fault features on the sub-basin floor may be important hosts for hydrothermal mineralization. These areas could be good for mineral exploration. The sedimentary basin thickness (1.2 km) is insufficient for hydrocarbon maturation because the minimum thickness for hydrocarbon concealment is approximately 2.3 km. This means that storing hydrocarbons in the area is out of the question.

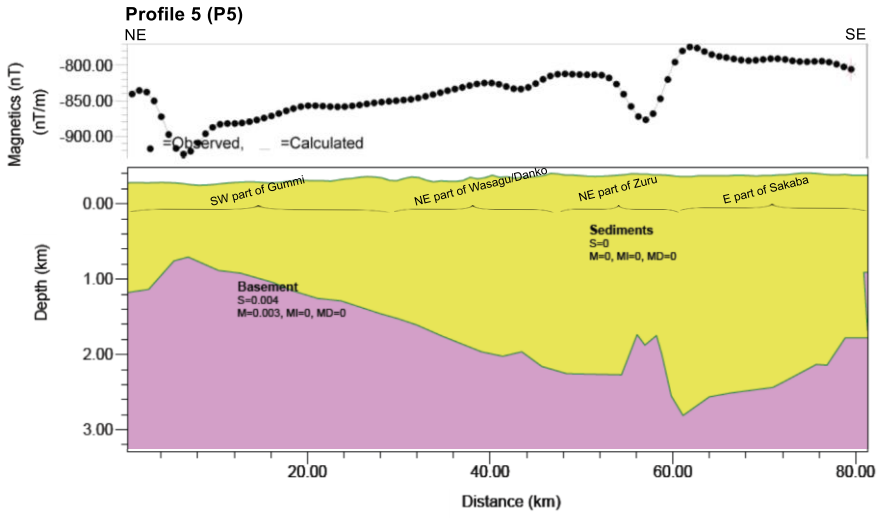

Fig. 12. 2D Iterative inversion model of magnetic data for profile five

5.4.5. POSSIBLE MINERALIZED ZONES OF THE STUDY AREA

Figure 13 shows the mineralization potential zones of the study area. These zones show the fracture curves with high magnetic anomalies along the 2D modelling profiles (P1, P2, P3, P4, and P5). The curve's pattern is usually caused by faults or shear zones. Fault features on the sub-basin floor may be important hosts for hydrothermal mineralization in these fault-induced areas. These areas may be suitable for mineral exploration. As

shown in Fig. 13, the areas corresponding to the Ngaski, Shanga, Rijau, Magma, Zuru, the eastern part of Yauri, and Kontagora.

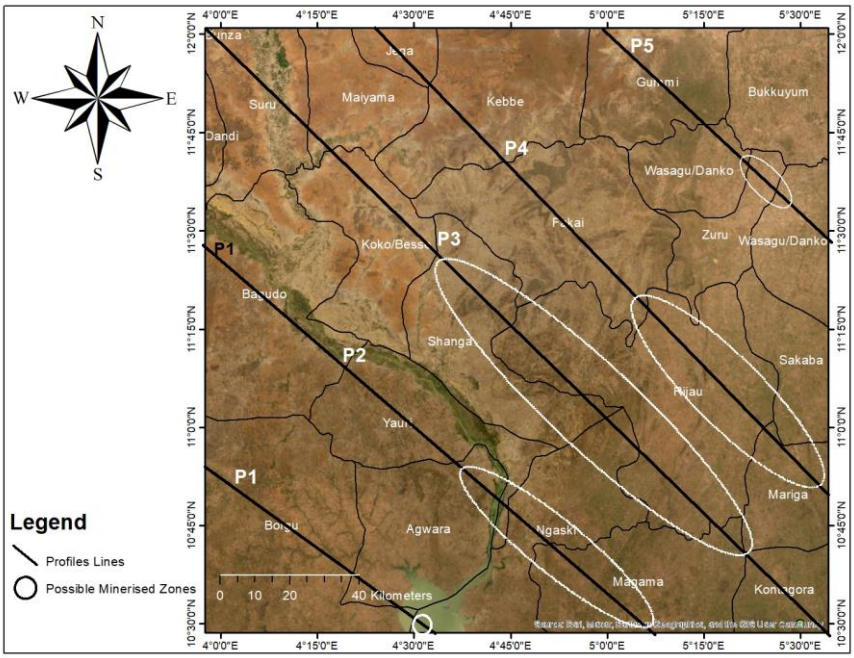

Fig. 13. Mineralization potential zones of the study area

6. CONCLUSIONS

The results of this study, which used the TDR technique and 2D forward modelling, revealed potential mineralization areas. This is significant and consequently an improvement in some earlier studies in the same area. The horizontal location and extent of the edges of various magnetic sources that formed lineaments are revealed by TDR. The shallow and deep sources of magnetic anomalies had more pronounced edges. The major structures were discovered in the SE part of Yauri and Shanga, Fakai, Ngaski, Zuru, Magama, Rijau, Wasagu/Danko, and Bukkuyum. The 2D modelling of magnetic data for the selected profiles (PI, P2, P3, P4, and P5) identifies zones with a high magnetic anomaly responding to fractures. The selected profiles' subsurface features are essentially sediments and the basement. For P1, P2, P3, P4, and P5, the maximum depth/thickness of the sediment section that crossed the sedimentary basin is 1.4 km, 1.5 km, 0.8 km, 1.2 km, and 1.2 km, respectively. The depth/thickness of the sediment section that crossed the basement complex zone is 1.8 km, 2.6 km, 9.6 km, 2.9 km, and 2.6 km for

P1, P2, P3, P4, and P5. In comparison to the SPI results, the depth/thickness of the sediments that crossed the areas of the sedimentary basin and basement complex zones is 1.671 km and <0.137 km, respectively. Due to various impediments, the SPI results did not match the results of 2D forward modeling. It only provides an average depth of magnetic source and is unable to accurately map the undulating basement. This explains why, in this study, 2D forward modelling was used to provide sediment thickness while accurately reflecting basement topography. In a portion of the sedimentary basin, the obtained thickness/depth of the sediments is insufficient for hydrocarbon maturation. The minimum thickness for the concealment of hydrocarbons, according to Wright et al. (1985), is about 2.3 km; the results obtained fall short of this standard. This implies that accumulating hydrocarbons is not a viable option. Fault/shear zones may have caused the fracture regions in the basement complex area. The regions are underlain by quartz-mica schist, biotite-hornblende, granite, biotite, gneiss, diorite, migmatite, medium coarse-grained sandstone, ironstones, laterite, siltstones, and clay in comparison to the geological setting. Fault features on the sub-basin floor may be important hosts for hydrothermal mineralization in these fault-induced areas. These areas may be suitable for mineral exploration. Potential mineralization zones were discovered to correspond to the Ngaski, Shanga, Rijau, Magma, Zuru, eastern part of Yauri, and Kontagora. The use of magnetic data analyses in this study has aided in mapping the lineaments (such as faults, fractures, or shear zones) thought to be associated with alteration zones, which play an important role in determining mineralization potential zones.

REFERENCES

ADAMA M., ABU M., and NAEEM A.N., 2019, *2D-Modeling of the major structures within the Chad Basin, Nigeria, from aeromagnetic data*, International Journal of Science and Research Methodology, 12 (4), 99–113.

ADETONA A.A., SALAKO K.A., and RAFIU A.A., 2018, *Delineating the lineaments within the major structures around eastern part of Lower Benue Trough from 2009 aeromagnetic data*, FUW Trends in Science and Technology Journal, 3 (1), 175–179.

ADEWUMI T. and SALAKO K.A., 2018, *Delineation of mineral potential zone using high resolution aeromagnetic data over part of Nasarawa state, north central, Nigeria*, Egyptian Journal of Petroleum, 27 (4), 759–767, https://doi.org/10.1016/j.ejpe.2017.11.002

AUGIE A.I., SALAKO K.A., RAFIU A.A., and JIMOH M.O., 2021, *Estimation of depth to structures associated with gold mineralisation potential over southern part of Kebbi state using aeromagnetic data*. [in:] Federal University of Technology Minna, 3rd School of Physical Sciences Biennial International Conference, Futminna 2021, 290–297.

AUGIE A.I., SALAKO K.A., RAFIU, A.A., and JIMOH M.O., 2022, *Geophysical assessment for gold mineralization potential over the southern part of Kebbi state using aeromagnetic data*, Geology, Geophysics and Environment, 48 (2), 177–193, https://doi.org/10.7494/geol.2022.48.2.177

BLAKELY R.J., 1996, *Potential theory in gravity and magnetic application*, Cambridge University Press, Cambridge, pp. 441.

BONDE D.S., LAWALI S., and SALAKO K.A., 2019, *Structural mapping of solid mineral potential zones over southern part of Kebbi state, northwestern Nigeria*, Journal of Scientific and Engineering Research, 6 (7), 229–240.

CORE D., BUCKINGHAM A., and BELFIELD S., 2009, *Detailed structural analysis of magnetic data-done quickly and objectively*, SGEG Newsletter, 1 (2), 15–21.

DANBATTA U.A., 2008, *Precambrian crustal development in the north-western part of Zuru schist belt, northwestern Nigeria*. Journal of Mining and Geology, 44 (1), 43–56. https://doi.org/10.4314/jmg.v44i1.18883

EJEPU J.S., UNUEVHO C.I., AKO T.A., and ABDULLAHI S., 2018, *Integrated geosciences prospecting for gold mineralization in Kwakuti, north-central Nigeria*, Journal of Geology and Mining, 10 (7), 81–94, https://doi.org/10.5897/JGMR2018.0296

HOLDEN E.J., DENTITH M., and KAVESI P., 2008, *Towards the automatic analysis of regional aeromagnetic data to identify regions prospective for gold deposits*, Computer Geoscience, 34, 1505–1513, https://doi.org/10.1016/j.cageo.2007.08.007

ISLES D.T and RANKIN L.R., 2013, *Geophysical interpretation of aeromagnetic data*, Australian Society of Exploration Geophysicist, CSIRO Publishing, 150, Oxford Street, Collingwood VIC 3066, Austria.

LAWAL M.M., SALAKO K.A., ABBAS M., ADEWUMI T., AUGIE A.I., and KHITA M., 2021, *Geophysical investigation of possible gold mineralization potential zones using a combined airborne magnetic data of lower Sokoto basin and its environs, northwestern Nigeria*, International Journal of Progressive Sciences and Technologies (IJPSAT) 30 (1), 1–16.

LAWALI S., SALAKO K.A., and BONDE D.S., 2020, *Delineation of mineral potential zones over lower part of Sokoto basin, northwestern Nigeria using aeromagnetic data*, Academic Research International, 11 (2), 19–29.

MAGHFIRA P.D. and NIASARI S.W., 2017, *Magnetic data analysis to determine the subsurface structures in Candiumbul geothermal prospect area, central java*, American Institute of Physics (AIP) Conference Proceedings 1861, 030041, https://doi.org/10.1063/1.4990928

MILLER H.G. and SINGH V.J., 1994, *Potential field tilt: a new concept for location of potential field sources*, Applied Geophysics, 32, 213–217, https://doi.org/10.1016/09269851(94)90022-1

NGSA, 2006, Nigerian Geological Survey Agency.

ODIDI I.G., MALLAM A., and NASIR N., 2020, *Depth to magnetic sources determination using source parameter imaging (SPI) of aeromagnetic data of parts of central and north-eastern Nigeria: a reconnaissance tool for geothermal exploration in the area*, Science World Journal, 15 (3), 19–23.

PHAM L.T., 2021, *A high resolution edge detector for interpreting potential field data: a case study from the Witwatersrand basin, South Africa*, Journal of African Earth Sciences, 178, https://doi.org/10.1016/j.jafrearsci. 2021.104190

PHAM L.T., OKSUM E., DO T.D., LE-HUY M., VU M.D., and NGUYEN V.D., 2019, *LAS: A combination of the analytic signal amplitude and the generalized logistic function as a novel edge enhancement of magnetic data*, Contributions to Geophysics and Geodesy, 49(4), 425–440. https://doi.org/10.2478/congeo-2019-0022

PHAM L.T., OKSUM E., LE D.V., FERREIRA F.J.F., and LE S.T., 2021, *Edge detection of potential field sources using the softsign function*, Geocarto International. https://doi.org/10.1080/10106049.2021.1882007

PHAM L.T., VU T.V., THI S.L., *Trinh and P.T. (2020). Enhancement of potential field source boundaries using an improved logistic filter*, Pure and Applied Geophysics, 177, 5237–5249, https://doi.org/10.1007/s00024-020-02542-9.

RAMADAN T.M. and ABDELFATTAH M.F., 2010, *Characterization of gold mineralization in garin hawal area, kebbi state, nw nigeria, using remote sensing*, Egyptian Journal of Remote Sensing and Space Science, 13 (2), 153–163, https://doi.org/10.1016/j.ejrs.2009.08.001

REEVES C., 2005, *Aeromagnetic surveys: principles, practice and interpretation*, Earthworks-Global Thinking in Exploration Geoscience, Geosoft.

TALWANI M. and HEIRTZLER J.R., 1964, *Computation of magnetic anomalies caused by two dimensional structures of arbitrary shape in computers in the mineral industries*, Geological Sciences, 9, 464–480.

TALWANI M., SUTTON G.H., and WORZEL J.L., 1959, *A crustal section across the Puerto Rico trench*, Journal of Geophysical Research, 64 (10), 1545–1555.

THOMPSON D.T., 1982, *EULDPH: A new technique for making computer-assisted depth estimates from magnetic data*, Geophysics, 47 (1), 31–37, https://doi.org/10.1190/1.1441278

THURSTON J.B. and SMITH R.S., 1997, *Automatic conversion of magnetic data to depth, dip and susceptibility contrast using the SPITM method*, Geophysics, 62 (3), 807–813, https://doi.org/10.1190/1.1444190

WRIGHT J.B., 1985, *Geology and mineral resources of West Africa*, Science, 58–59, https://doi.org/10.1002/gj.3350220519